Article:

de Carvalho, C.F., Planidin, N.P., Villoutreix, R. et al. (2025) Linking DNA methylation to localised genetic differentiation in Timema cristinae stick insects. Molecular Ecology, 34 (22). e70049. ISSN: 0962-1083

https://doi.org/10.1111/mec.70049

Supporting Information for

Linking DNA methylation to genetic differentiation in *Timema cristinae* stick insects

Authors: Clarissa F. de Carvalho[1,†*], Nicholas P. Planidin[2], Romain Villoutreix[2], Víctor Soria-Carrasco[3], Rüdiger Riesch[2,4], Jeffrey L. Feder[5], Jon Slate[1], Patrik Nosil[1,2,], Zachariah Gompert[6]

Affiliations:

[1]School of Biosciences, University of Sheffield; Sheffield, S10 2TN, UK
[2]SETE, Univ Université Paul Sabatier, CNRS, UMR-5321, F-09200 Moulis, France
[3]John Innes Centre; Norwich, NR4 7UH, UK
[4]Department of Biological Sciences, Centre for Ecology, Evolution and Behaviour, Royal Holloway University of London; Egham, TW20 0EX, UK.
[5]Department of Biological Sciences, University of Notre Dame, Notre Dame, Indiana, 46556, USA
[6]Department of Biology, Utah State University; Logan, Utah, 84322, USA
†*Present address: Departamento de Ecologia e Biologia Evolutiva, UNIFESP; Diadema, 09972-270, Brazil*
**Corresponding authors*

Email: clarissa.carvalho@unifesp.br

This PDF file includes:

Figures S1 to S12
Tables S1 to S3

Supplementary Text

Population overlap between epigenomic and genomic datasets

There was near-complete overlap between the populations analyzed with whole-genome bisulfite sequencing (WGBS; de Carvalho et al., 2023) and those with the whole-genome sequencing dataset (WGS; Soria-Carrasco et al., 2014) used in this study. The only exceptions were the populations from MR and R12 (WGS), which are not included in WGBS (Fig. 2). However, the population from MR is just 300m from the populations at N1 (included in WGBS), and shares similar ecological conditions, as evidenced by nearly identical proportion of host plants (exemplified by the %striped individuals in MR=48.3% and in N1=46.8%; Wilcoxon rank-sum test W = 18, p-value = 1; based on the dataset from Nosil et al., 2018). This suggests strong genetic similarity between populations from MR and N1.

In contrast, the R12 populations (R12A and R12C) are geographically distant from most WGBS-sampled populations, being located in a different mountain. We retained them in our study to include population pairs with higher degrees of divergence. To evaluate whether the results on geographical pattern of F_{ST} enrichment in DMRs (one of our core findings) depend on R12, we repeated the F_{ST} analyses after excluding these populations.

Using the same approach as described in the main text, we assessed F_{ST} enrichment in DMRs, and tested its association with log-transformed geographical distances using Mantel tests with the R package *vegan* v2.6-6.1 (Oksanen et al., 2022). This was done for both all DMRs and genic DMRs. The results remained robust: F_{ST} enrichment in DMRs increased significantly with geographical distance for all DMRs (Mantel r = 0.71, P = 0.031) and genic DMRs (r = 0.69, P = 0.036), even without R12. These results indicate that the greater enrichment of F_{ST} in DMRs is not driven by outliers arising from R12 populations, but reflects a broader trend across *T. cristinae* populations.

Overlap between DMRs and top 5% F_{ST} regions

To complement the results that DMRs exhibit greater F_{ST} than expected by chance (Figs. S1-S3), we tested whether DMRs were enriched in regions with the most accentuated F_{ST} in the distribution. To this end, we calculated the average pairwise F_{ST} across all 28 population pairs, and selected the top 5% of the upper tail of the mean F_{ST} distribution. We then tested whether DMRs delimited by the P<0.0004 – the 0.04th percentile of the *p-value* empirical distribution – were enriched in these most accentuated F_{ST} regions. The F_{ST} threshold for these top 5% values varied 0.05 to 0.85 depending on the degree of genetic differentiation between each population pair.

In addition, for each population pair, we assessed how many DMRs (P<0.0004) overlapped with regions with top 5% F_{ST} values. Statistical significance for both analysis was again estimated using randomization tests that permuted F_{ST} values across loci 1,000 times to generate null expectations. These analyses were conducted separately for both genome-wide and genic DMRs.

We found that 12% of DMRs overlapped with genomic regions in the top 5% of F_{ST} values – twice the proportion expected by chance (expected=5%), but at the edge of statistical significance (P=0.096; randomization test using mean F_{ST} across all comparisons). This trend was stronger and marginally more significant for genic DMRs, with 15% exhibiting accentuated F_{ST} (expected=5%; P=0.077; same randomization test; Fig. 3). Moreover, 5 out of 28 population pairs (18%) exhibited a significant overlap between the 1kbp tiles with top 5% F_{ST} values and in DMRs (P<0.050 for each pair), exceeding the expected frequency of 5% (*i.e.,* 1.4 comparisons; *P*=0.012). A similar pattern was observed for genic DMRs, with 4 out of 28 comparisons (14%) showing significant overlap (expected=5%, *P*=0.012).

Climatic variation across T. cristinae *populations*

The first two principal components explained around 92% of the variance (PC1=66.4%, PC2=25.5%). PC1 reflects annual temperatures, as well as temperatures during the coldest and wettest periods,and also captures temperature constancy across the seasons (e.g. isothermality, seasonality). PC2 primarily represents temperatures in the warmest month, and in the warmest and driest quarters (see also de Carvalho et al., 2023). Among the populations studied, LA, MR1A and MR1C are found in regions with highest precipitation indices, while R12A and R12C are located in drier regions and with higher isothermality. HVA, HVC and PRC are located in regions with highest temperatures during the warmest and driest quarters (Fig. S4). These climatic and host-plant variations were used to test the hypothesis that F_{ST} enrichment within DMRs is associated with these factors.

Testing for DMRs occurring in gene-dense genomic regions

We examined whether DMRs were located in gene-dense regions. If this were the case, there would be higher chances of existing genes under natural selection in LD with a DMR, which could thus elevate F_{ST} in the DMR through genetic hitchhiking. However, our analyses showed no significant differences in gene counts between DMRs and non-DMR methylation tiles in 20 kbp and 100 kbp genomic windows. These window sizes were chosen to span a biologically plausible range for LD in *Timema* and related systems (Edelman et al., 2019; Martin et al., 2013; Riesch et al., 2012), with 20 kbp reflecting relatively tight linkage and 100 kbp allowing for more distal associations. The median difference in gene counts was 0 in both cases (*P* =0.999 and *P*=0.981, permutation tests). These results suggest that gene density cannot explain F_{ST} enrichment in DMRs.

Supplementary Figures

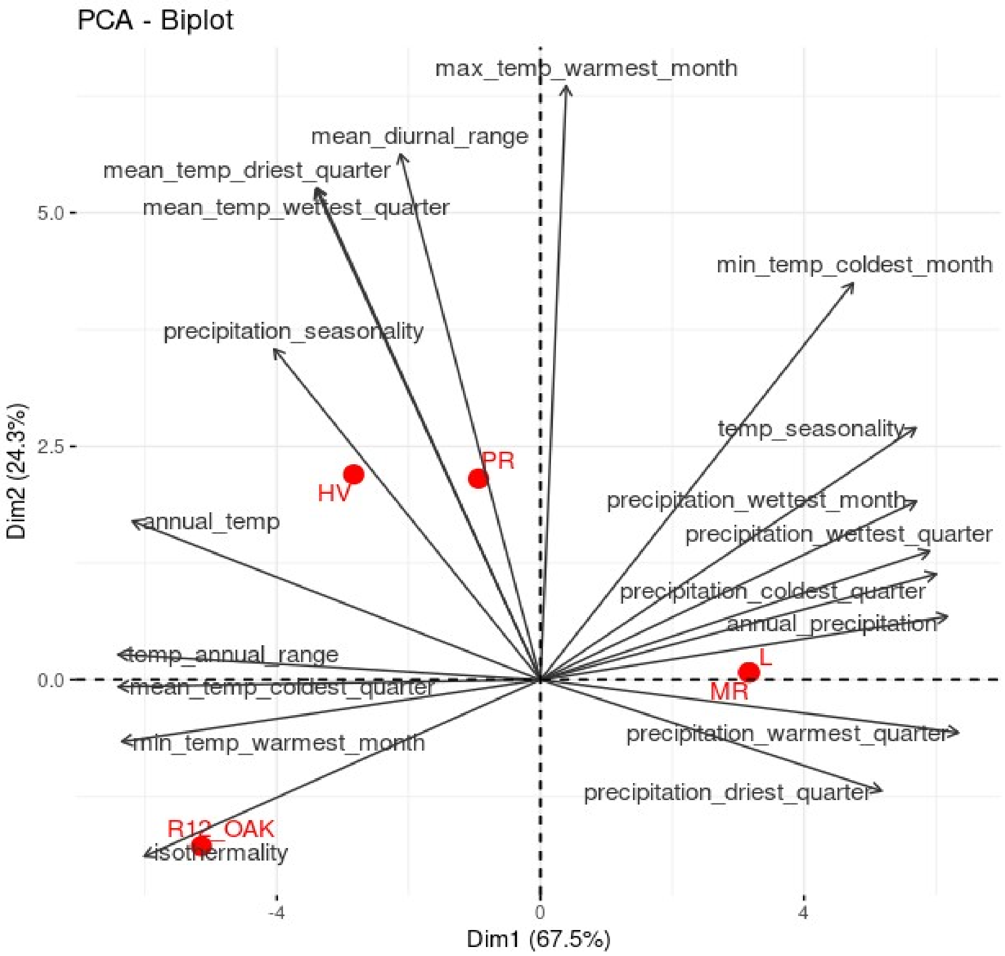

Figure S1. First two principal components (PC) on Worldclim bioclimatic variables represented for the *T. cristinae* localities used in this study. PC analysis was performed using all recorded sites in a previous study (Nosil et al., 2018). Both PC1 and PC2 are strongly correlated with elevation. Abbreviations: annual_temp = annual mean temperature, temp_seasonality = temperature seasonality, max_temp_warmest_month = maximum temperature of the warmest month, min_temp_warmest_month = minimum temperature of the warmest month, min_temp_coldest_month = minimum temperature of the coldest month, temp_annual_range = temperature annual range, mean_temp_wettest_quarter = mean temperature of the wettest quarter, mean_temp_driest_quarter = mean temperature of the driest quarter, mean_temp_coldest_quarter = mean temperature of the coldest quarter.

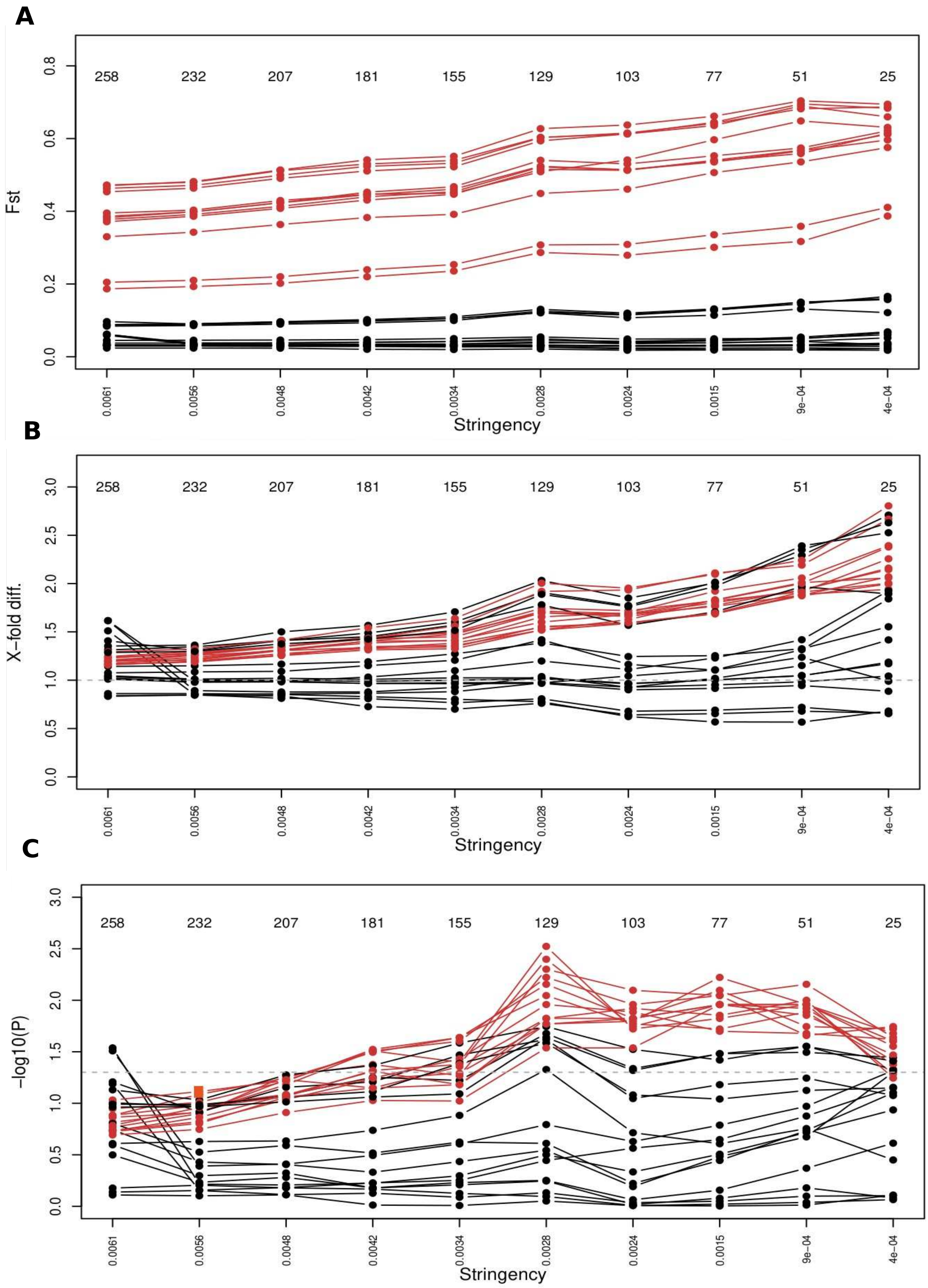

Fig. S2. F_{ST} in DMRs among all pairs of populations across different p-value cut-offs delimiting DMRs. Colors denote pairwise comparisons within the same (black) or between different mountains (red), the latter denoting a marked geographical separation. (**A**) Pairwise F_{ST} along different stringency level of p-value cut-offs, estimated based on the empirical p-value distributions (from the 0.4% percentile to the 0.04% smallest p-values). (**B**) ‘X-fold diff.’ expresses, at each population pair, the mean F_{ST} in DMRs relative to null expectations. (**C**) P-value of significance between observed levels of F_{ST} in DMRs compared to the background levels (represented by the dashed line). Numbers at the top represent the number of DMRs.

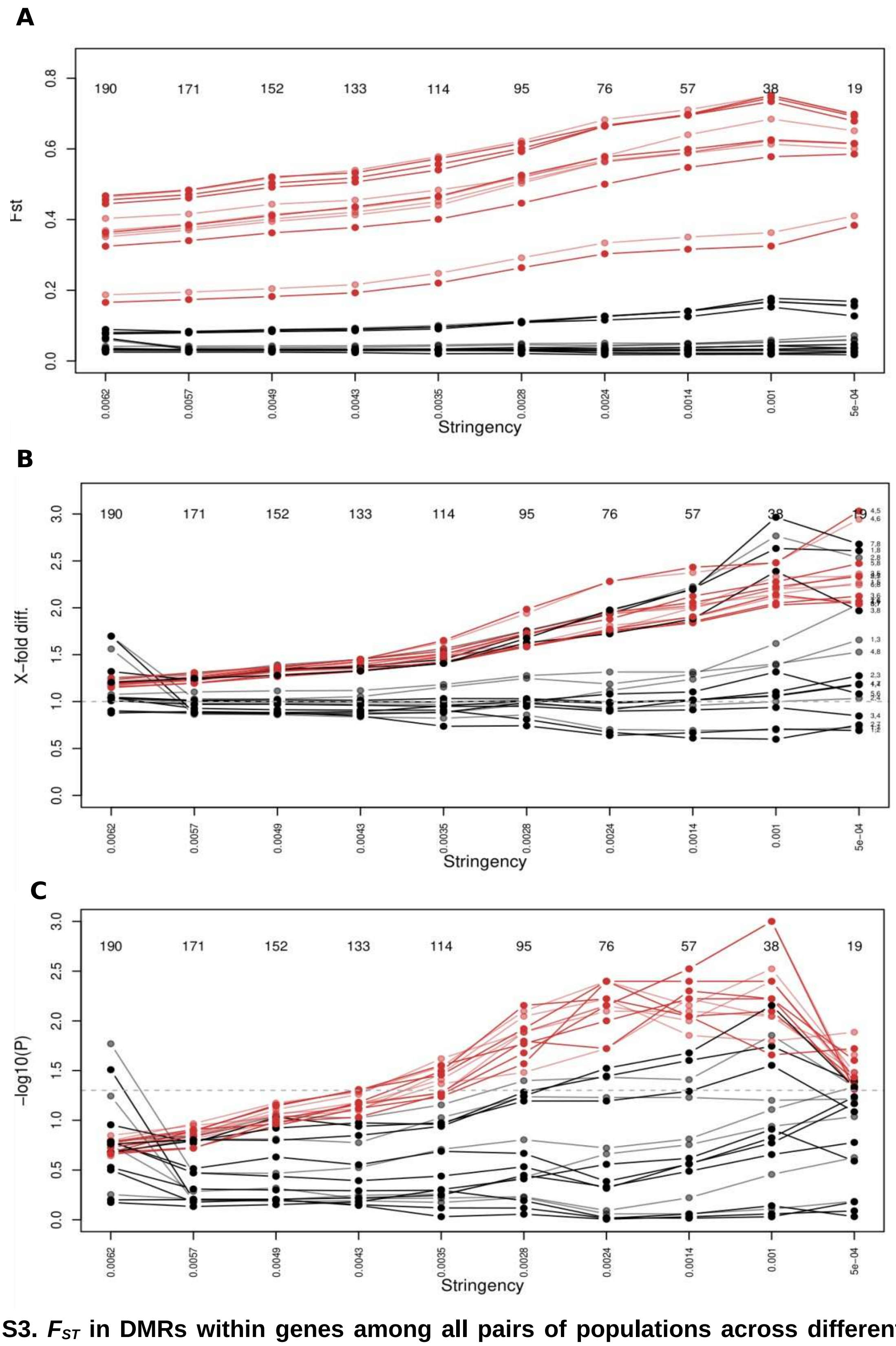

Fig. S3. F_{ST} in DMRs within genes among all pairs of populations across different p-value cut-offs delimiting DMRs. Colors denote pairwise comparisons within the same (black) or between different mountains (red), the latter denoting a marked geographical separation. (**A**) Pairwise F_{ST} along different stringency level of p-value cut-offs, estimated based on the empirical p-value distributions (from the 0.4% percentile to the 0.04% smallest p-values). (**B**) A'X-fold diff.' expresses, at each population pair, the mean F_{ST} in DMRs relative to null expectations. (**C**) P-value of significance between observed levels of F_{ST} in genic DMRs compared to the background levels (represented by the dashed line). Numbers at the top represent the number of DMRs.

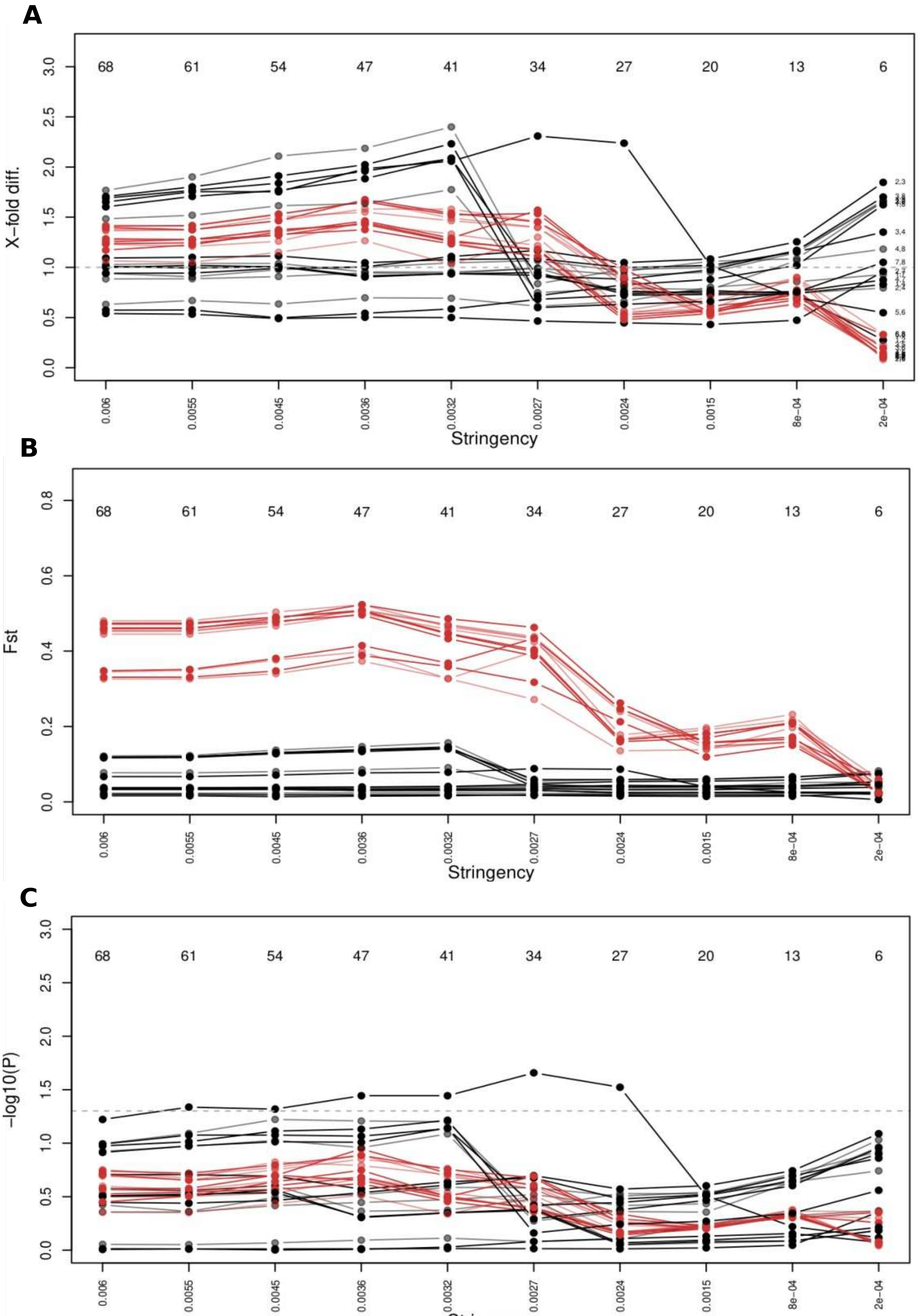

Fig. S4. F_{ST} in DMRs outside genes among all pairs of populations across different p-value cut-offs delimiting DMRs. Colors denote pairwise comparisons within the same (black) or between different mountains (red), the latter denoting a marked geographical separation. (**A**) 'X-fold diff.' expresses, at each population pair, the mean F_{ST} in DMRs relative to null expectations. (**B**) Pairwise F_{ST} along different stringency level of p-value cut-offs, estimated based on the empirical p-value distributions (from the 0.4% percentile to the 0.04% smallest p-values). (**C**) P-value of significance between observed levels of F_{ST} in intergenic DMRs compared to the background levels (represented by the dashed line). Numbers at the top represent the number of DMRs at each p-value cut-off

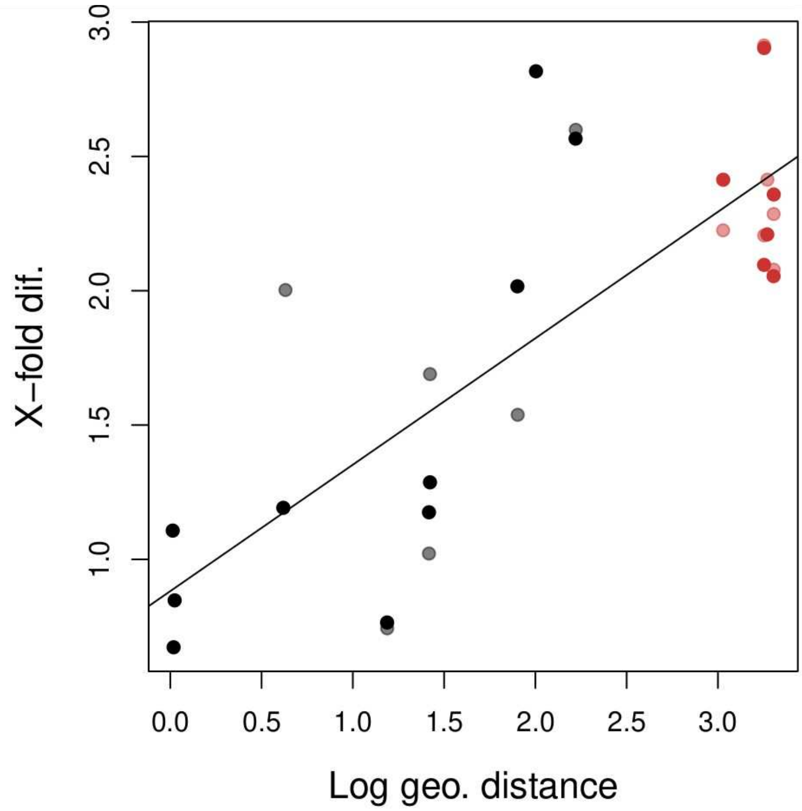

Fig. S5. Mean F_{ST} in genic DMRs relative to null expectations progressively getting higher with geographical distance relative to genomic background. 'X-fold diff.' expresses F_{ST} enrichment in DMRs compared to the background levels. Colors denote pairwise comparisons within the same (black) or between different mountains (red), the latter denoting a marked geographical separation. Solid points represent different hosts, and more transparent points represent same hosts (R^2=0.57, P=0.001; Mantel test).

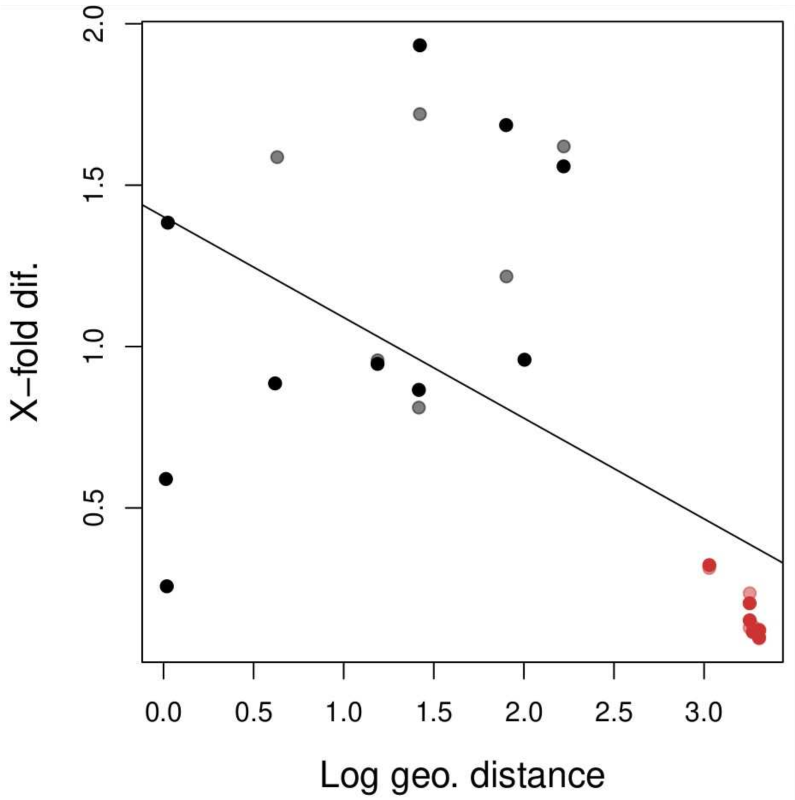

Fig. S6. Mean F_{ST} in non-genic DMRs relative to null expectations and geographical distance between populations. 'X-fold diff.' expresses F_{ST} enrichment in DMRs compared to the background levels. Colors denote pairwise comparisons within the same (black) or between different mountains (red), the latter denoting a marked geographical separation. Solid points represent different hosts, and more transparent points represent same hosts (R^2=0.14; P=0.963; Mantel test).

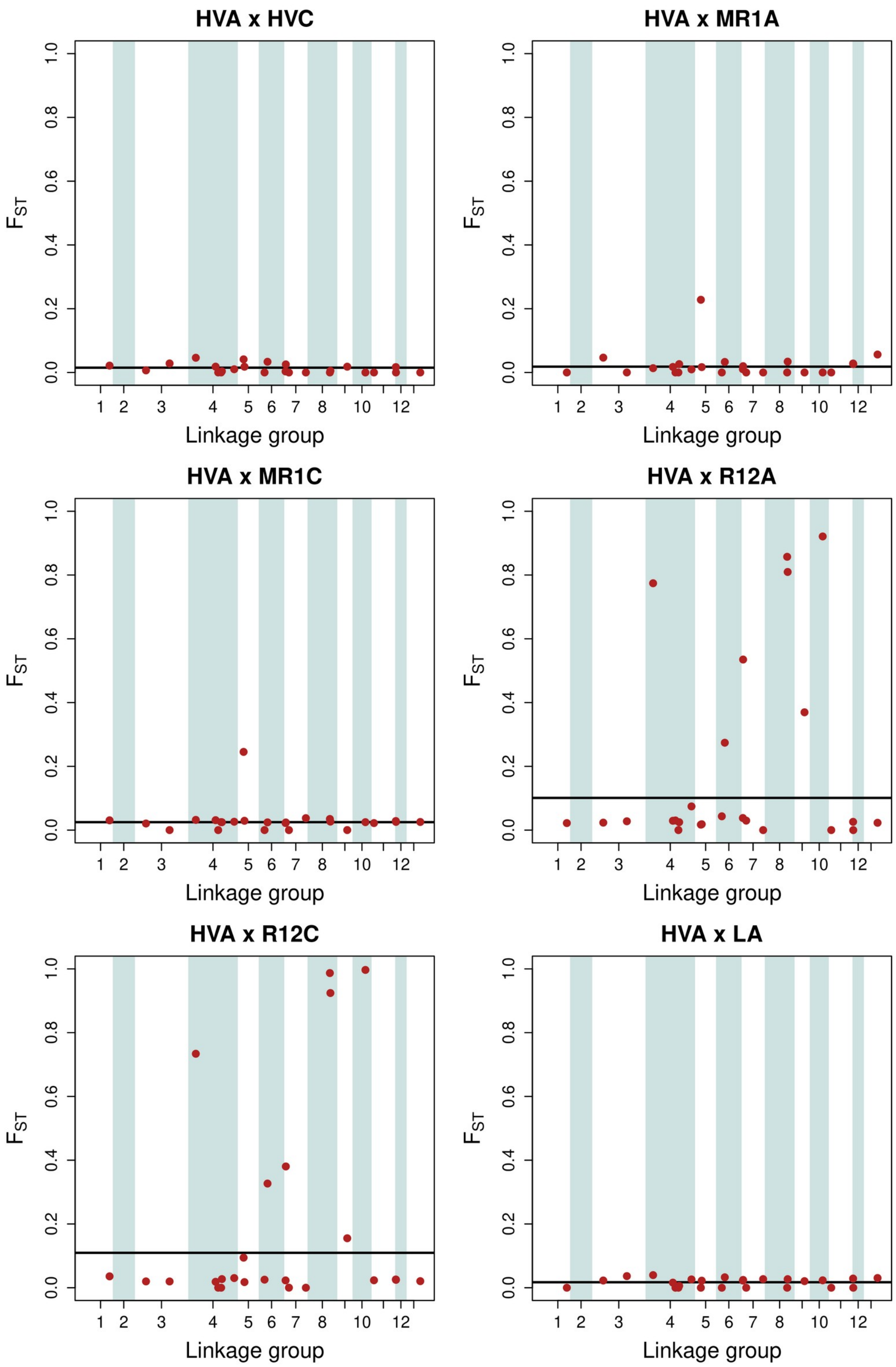

Fig. S7. F_{ST} values in DMRs between some representative population pairs separated by different degrees of geographical isolation. The black bar represents the mean F_{ST} across methylation tiles (null expectation) and the red dots represent the F_{ST} in DMRs. DMRs tend to exhibit higher F_{ST} values with increasing levels of geographic isolation, but not necessarily being host dependent. DMRs here are delimited by $P < 0.0006$.

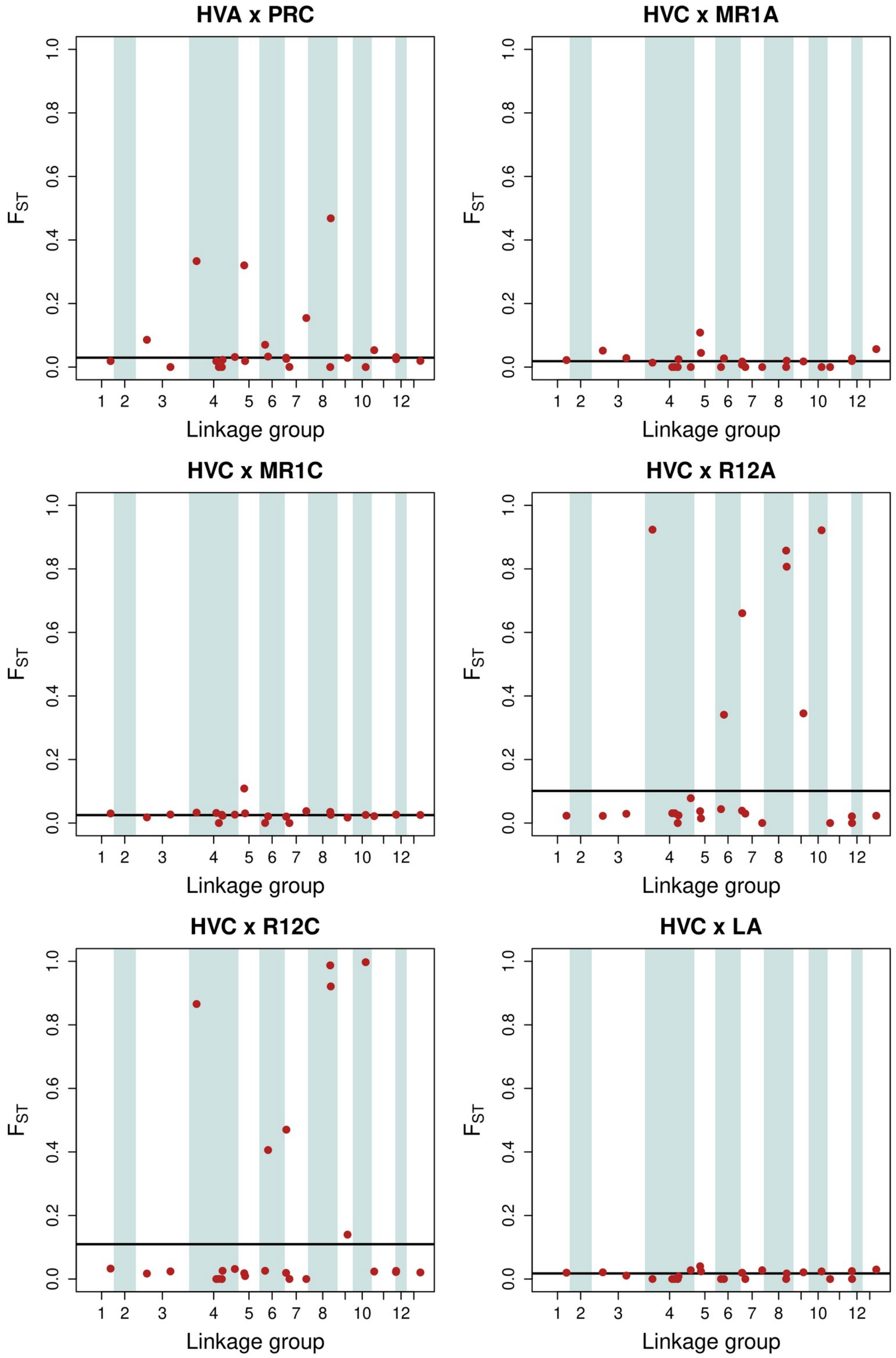

Fig. S8. F_{ST} values in DMRs between some representative population pairs separated by different degrees of geographical isolation. The black bar represents the mean F_{ST} across methylation tiles (null expectation) and the red dots represent the F_{ST} in DMRs. DMRs tend to exhibit higher F_{ST} values with increasing levels of geographic isolation, but not necessarily being host dependent. DMRs here are delimited by $P < 0.0006$.

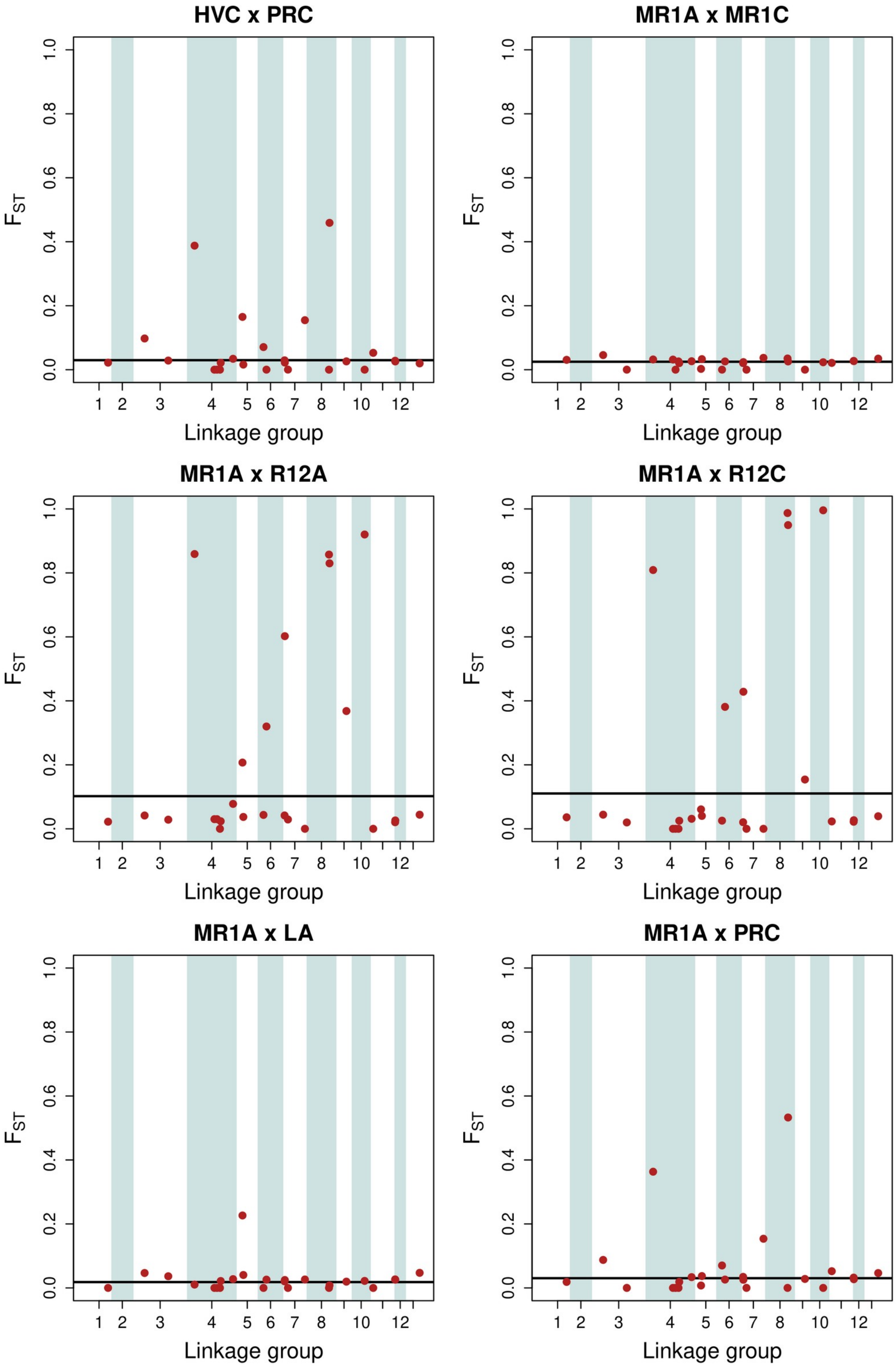

Fig. S9. F_{ST} values in DMRs between some representative population pairs separated by different degrees of geographical isolation. The black bar represents the mean F_{ST} across methylation tiles (null expectation) and the red dots represent the F_{ST} in DMRs. DMRs tend to exhibit higher F_{ST} values with increasing levels of geographic isolation, but not necessarily being host dependent. DMRs here are delimited by $P < 0.0006$.

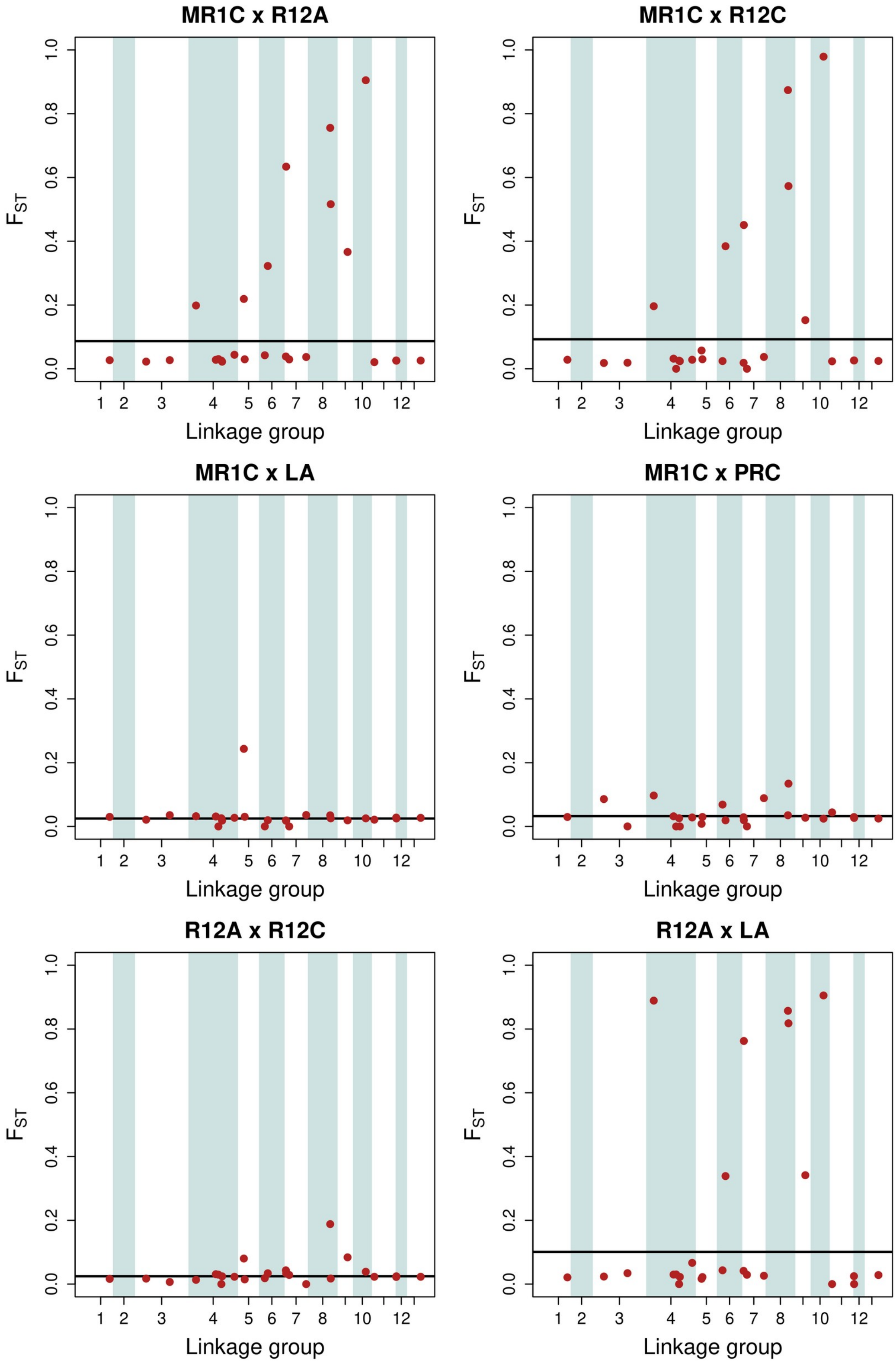

Fig. S10. F_{ST} values in DMRs between some representative population pairs separated by different degrees of geographical isolation. The black bar represents the mean F_{ST} across methylation tiles (null expectation) and the red dots represent the F_{ST} in DMRs. DMRs tend to exhibit higher F_{ST} values with increasing levels of geographic isolation, but not necessarily being host dependent. DMRs here are delimited by $P < 0.0006$.

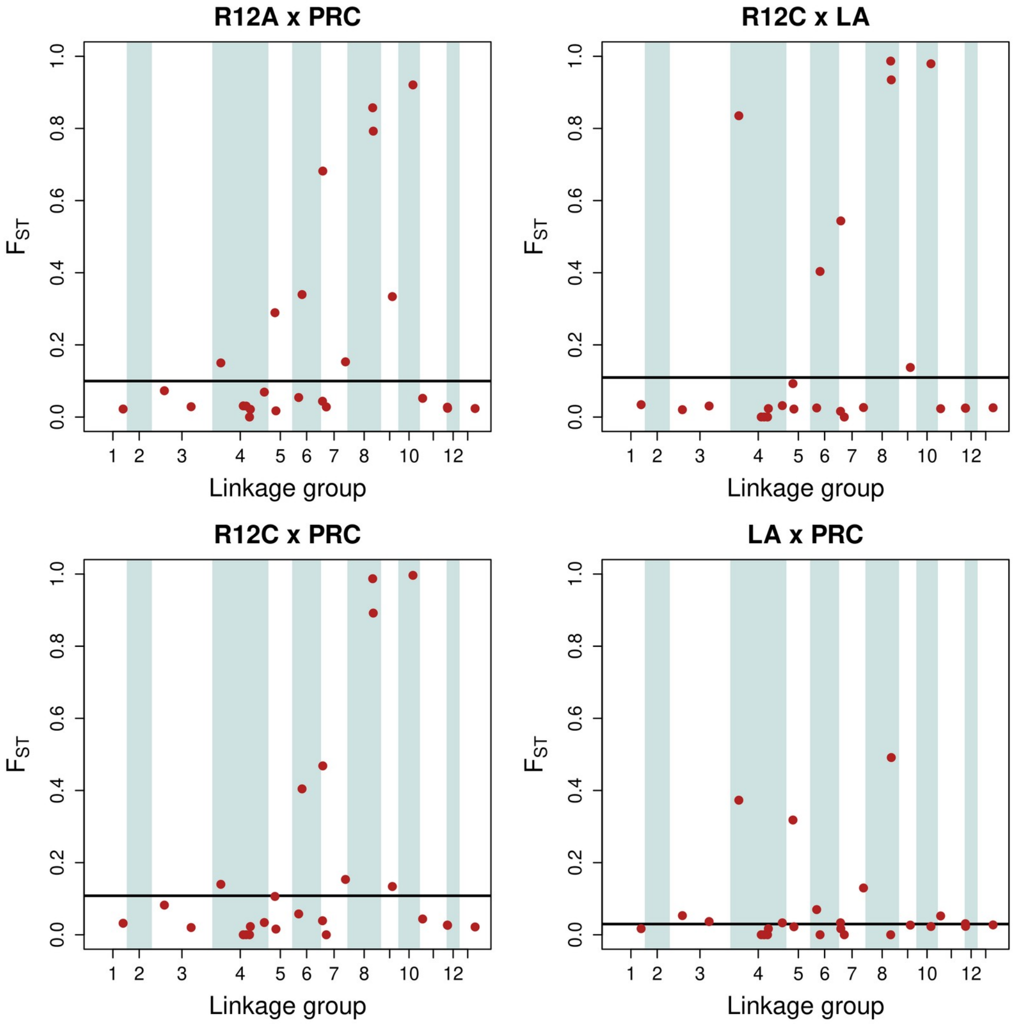

Fig. S11. F_{ST} values in DMRs between some representative population pairs separated by different degrees of geographical isolation. The black bar represents the mean F_{ST} across methylation tiles (null expectation) and the red dots represent the F_{ST} in DMRs. DMRs tend to exhibit higher F_{ST} values with increasing levels of geographic isolation, but not necessarily being host dependent. DMRs here are delimited by $P < 0.0006$.

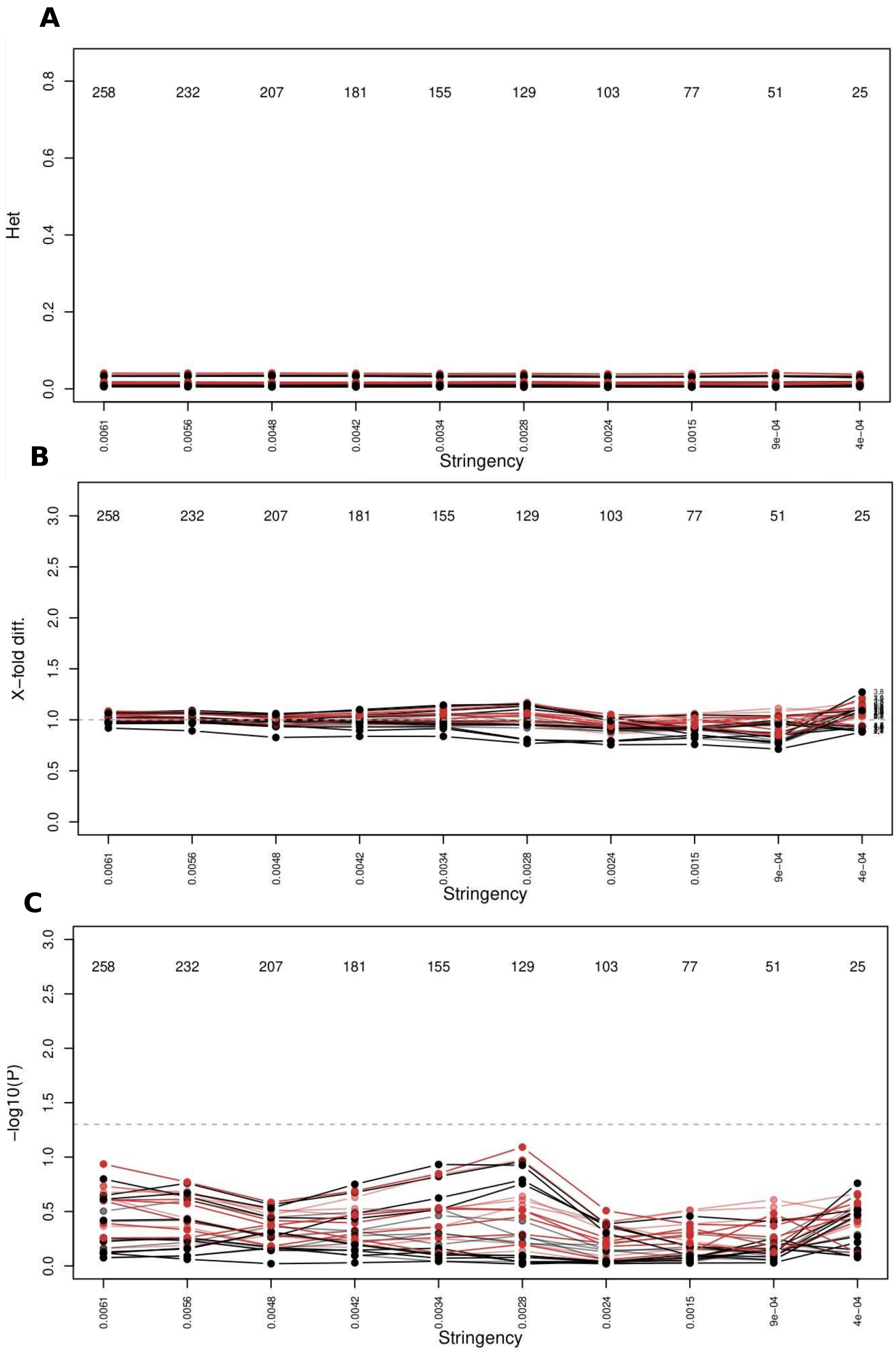

Fig. S12: Heterozygosity (*Het*) in DMRs among all pairs of populations across different p-value cut-offs. Colors denote pairwise comparisons within the same (black) or between different mountains (red), the latter denoting a marked geographical separation. (**A**) Pairwise *Het* along different stringency level of p-value cut-offs, estimated based on the empirical p-value distributions (from the 0.4% percentile to the 0.04% smallest p-values). (**B**) Accentuation of *Het*; X-fold difference expresses relative *Het* values in DMRs compared to the background levels. (**C**) P-value of significance between observed levels of *Het* in DMRs compared to the background levels (represented by the dashed line).

Supplementary Tables

Table S1. Summary of model comparison evaluating the possible effects of geographic distance (G), host distance (H), climate PC1 and PC2 distance on the log ratio of observed to expected genetic differentiation (*F_{ST}*) for DMRs. Deviance = mean deviance, pD = effective number of parameters, DIC = deviance information criterion, and ΔDIC = change in DIC relative to the top model. Models are sorted by DIC (from lowest = best to highest = worst).

Model	**Deviance**	**pD**	**DIC**	**ΔDIC**
G + PC1	53.33	6.82	60.14	0
G + PC1 + PC2	54.47	7.72	62.19	2.05
G + H + PC1	54.65	7.73	62.38	2.24
G	57.49	5.52	63.01	2.87
G + H + PC1 + PC2	55.66	8.62	64.27	4.13
G + PC2	58.50	6.13	64.63	4.49
G + H	58.87	6.55	65.41	5.27
G + H + PC2	59.56	7.26	66.82	6.68
PC2	65.95	4.40	70.35	10.21
PC1 + PC2	66.84	5.49	72.33	12.19
H + PC2	67.00	5.48	72.48	12.34
H + PC1 + PC2	67.75	6.43	74.17	14.03
H	78.14	5.01	83.15	23.01
PC1	78.38	5.00	83.38	23.24
H + PC1	78.84	6.07	84.91	24.77

Table S2. Linkage disequilibrium (LD) within DMRs in each population based on whole-genome data. LD was calculated for each population using SNP genotypes within DMRs. LD distribution for DMRs was compared to a null distribution generated from random 1kbp windows (*i.e.,* enrichment of LD in DMRs, denoted by ‘effect’ in the table). The *p-values* were derived from 10,000 iterations in permutation tests.

location	**host**	**LD**	**effect**	***p-value***
HV	A	0.72	0.90	0.62
HV	C	0.68	0.87	0.71
MR1	A	0.63	0.74	0.88
MR1	C	0.64	0.88	0.70
R12	A	0.76	1.03	0.41
R12	C	0.79	1.07	0.28
L	A	0.88	1.27	0.07
PR	C	0.92	1.34	0.02

Table S3. Results of Mantel tests between F_{ST} values in C/T or G/A SNPs within DMRs between population comparsions and geographical distances between the populations. Reported below are the results with *p-value* < 0.05. Column 'CpG' represents whether the locus is located in CpG context or not (potential SNPs arisen from mutagenic effects).

locus	r	p-value	polymorphism	CpG
lg1_scaf1290:791133	**0.85**	**0.022**	**G/A**	**yes**
lg10_scaf4044:94527	0.86	0.020	G/A	no
lg10_scaf4044:94582	0.86	0.002	C/T	no
lg12_scaf1990:742684	0.35	0.039	C/T	no
lg4_scaf1314:35999196	0.35	0.044	G/A	no
lg4_scaf1314:74769144	0.35	0.021	G/A	no
lg4_scaf1314:74769479	0.65	0.008	G/A	no
lg6_scaf2778:26940748	0.76	0.011	G/A	no
lg8_scaf1465:3115902	0.87	0.019	G/A	no
lg9_scaf3246:101377	0.73	0.007	C/T	no

SI References

Edelman, N. B., Frandsen, P. B., Miyagi, M., Clavijo, B., Davey, J., Dikow, R. B., García-Accinelli, G., Van Belleghem, S. M., Patterson, N., Neafsey, D. E., Challis, R., Kumar, S., Moreira, G. R. P., Salazar, C., Chouteau, M., Counterman, B. A., Papa, R., Blaxter, M., Reed, R. D., … Mallet, J. (2019). Genomic architecture and introgression shape a butterfly radiation. *Science*, *366*(6465), 594–599. https://doi.org/10.1126/science.aaw2090

Martin, S. H., Dasmahapatra, K. K., Nadeau, N. J., Slazar, C., Walters, J. R., Simpson, F., Blaxter, M., Manica, A., Mallet, J., & Jiggins, C. D. (2013). Genome-wide evidence for speciation with gene flow in Heliconius butterflies. *Genome Research*, *23*, 1817–1828. https://doi.org/10.1101/gr.159426.113.

Nosil, P., Villoutreix, R., de Carvalho, C. F., Farkas, T. E., Soria-Carrasco, V., Feder, J. L., Crespi, B. J., & Gompert, Z. (2018). Natural selection and the predictability of evolution in Timema stick insects. *Science (New York, N.Y.)*, *359*(6377), Article 6377. https://doi.org/10.1126/science.aap9125

Oksanen, J., Simpson, G., Blanchet, F., Kindt, R., Legendre, P., Minchin, P., & et al. (2022). *The vegan package* [Computer software]. https://cran.r-project.org/package=vegan

Riesch, R., Barrett-Lennard, L. G., Ellis, G. M., Ford, J. K. B., & Deecke, V. B. (2012). Cultural traditions and the evolution of reproductive isolation: Ecological speciation in killer whales? *Biological Journal of the Linnean Society*, *106*(1), 1–17. https://doi.org/10.1111/j.1095-8312.2012.01872.x